FLOW OF TIME-DEPENDENT FLUIDS THROUGH A CYLINDER BETWEEN TWO PARALEL PLATES

Cleiton Fonseca, cfonseca@mecanica.ufrgs.br
Sergio L. Frey, frey@mecanica.ufrgs.br
Laboratory of Applied and Computational Fluid Mechanics (LAMAC), Department of Mechanical Engineering
Federal University of Rio Grande do Sul, Rua Sarmento Leite 425, RS 90050-170, Brazil

Mônica F. Naccache, naccache@puc-rio.br
Paulo R. de Souza Mendes, pmendes@puc-rio.br
Department of Mechanical Engineering, Pontifícia Universidade Católica do Rio de Janeiro
Rua Marquês de São Vicente 225, RJ 22453-900, Brazil

Abstract. A numerical analysis of a thixotropic fluid flowing through a cylinder between two parallel plates is performed, using the constitutive equation recently proposed by de Souza Mendes (2009). The constitutive equation couples viscoelasticity and viscoplasticity, by means of a fluid structure parameter. The conservation equations of mass and momentum coupled with the constitutive equation are solved via the finite element method, based on a four-field Galerkin least-squares formulation in terms of the extra-stress, pressure, velocity and structure parameter. The effect of a rheological parameter, the shear modulus, on the fluid structure and on the flow pattern is investigated in order to evaluate the model performance in complex flows.

Keywords*: Thixotropy, Structured fluids, modified UCM model, multi-field Galerkin least-squares method*

1. INTRODUCTION

A large class of non-Newtonian fluids has a microstructure leading to a elastic behavior for lower levels of stress. Above a critical stress value, the yield stress, this microstructure breaks, causing a steep decrease in elasticity and viscosity levels, together with a pseudoplastic fluid behavior. Moreover, these fluids may also present a time-dependent viscosity: the viscosity changes with the time of shearing. If the viscosity decreases with time as the fluid undergoes a shear rate increase in a reversible process, the fluid is called thixotropic (Barnes, 1997). These fluids can be frequently found both in nature and in industrial applications such as polymer melts and solutions, paints, mud, detergents, cosmetics, gels, creams and pastes, foods such as yogurt and fruit juices, and solutions of stabilizers and thickeners.

The aim of the present article is the numerical investigation of a thixotropic fluid flowing through a cylinder between two parallel plates, using the constitutive equation recently proposed by de Souza Mendes (2009). Interesting reviews of the thixotropic behavior of fluids are performed by Mewis and Wagner (2009) and Barnes (1997), where thixotropy and modelling are described and discussed. The model proposed by de Souza Mendes (2009) is a tentative equation to predict the thixotropic behavior of complex fluids. It is based on the upper-convected Maxwell constitutive equation for viscoelastic fluids, but with a relaxation time and viscosity function dependent on a structure parameter, which indicates the level of structure of the material. The time dependency is taken into account in the evaluation of the structure parameter, by means of an evolution equation.

The mechanical model is formed by the conservation equations of mass and momentum for incompressible fluids, coupled with the constitutive equation. In a first approximation, the temporal variation of the parameter structure shall be disregarded in the presence of terms accounting for its spatial advection and the buildup and breakdown of the material structure. Such an assumption leads to a simplification that transforms the equation of the structure parameter in a purely hyperbolic one, which certainly requires special care in its numerical approximation. The numerical approach is based on a four-field Galerkin least-squares formulation in terms of the extra-stress, pressure, velocity and structure parameter. This formulation is developed as an attempt to enhance the stability of the classical Galerkin approximation for differential viscoelastic flows, which major feature is to circumvent the compatibility conditions for the finite subspaces of primal variables, hence allowing the use of simple combinations of finite element interpolations, as the equal-order bilinear Lagrangian one. In addition, owing to an appropriate design of its least-squares mesh-dependent terms, this formulation remains stable even for locally elastic-dominated flows, where the upper-convected derivative of the material equation plays a relevant role. The effect of rheological parameters on the flow pattern and on the structure parameter is investigated and discussed. The ratio between the channel height and the cylinder diameter is held fixed and inertia is neglected. All the numerical results proved to be physically meaningful and in accordance with the related literature.

2. THE MODELING

In order to simulate creeping flows of thixotropic materials, a multi-field formulation composed by balance equations for mass and momentum, coupled with a thixotropic equation recently introduced by de Souza Mendes (2009), can be written as

$$\begin{aligned}
&\operatorname{div}\mathbf{u}=0 && \text{in } \Omega\\
&\operatorname{div}\boldsymbol{\tau}-\nabla p+\rho\mathbf{b}=\mathbf{0} && \text{in } \Omega\\
&\boldsymbol{\tau}+\theta(\lambda)\overset{\nabla}{\boldsymbol{\tau}}=2\eta_v(\lambda)\mathbf{D}(\mathbf{u}) && \text{in } \Omega\\
&\mathbf{u}\cdot\nabla\lambda=\frac{1}{t_{eq}}\left[(1-\lambda)^a-(1-\lambda_{ss})^a\left(\frac{\lambda}{\lambda_{ss}}\right)^b\left(\frac{\tau}{\eta_v(\lambda)\dot{\gamma}}\right)^c\right] && \text{in } \Omega\\
&\mathbf{u}=\mathbf{u}_g && \text{on } \Gamma_g^{\mathbf{u}}\\
&\boldsymbol{\tau}=\boldsymbol{\tau}_g && \text{on } \Gamma_g^{\boldsymbol{\tau}}\\
&\lambda=\lambda_g && \text{on } \Gamma_g^{\lambda}\\
&[\boldsymbol{\tau}-p\,\mathbf{1}]\mathbf{n}=\mathbf{t}_h && \text{on } \Gamma_h^{\boldsymbol{\tau}}\\
&\nabla\lambda\cdot\mathbf{n}=0 && \text{on } \Gamma_h^{\lambda}
\end{aligned} \tag{1}$$

where **u** is the velocity vector, p is the hydrostatic pressure and $\boldsymbol{\tau}$ is the extra-stress tensor, ρ is the fluid density, θ is the fluid relaxation time that depends on the structure parameter λ, **D** is the strain rate tensor, **b** is the body force per mass unit, t_{eq} is a characteristic time of change of the parameter λ, a, b and c are positive scalar coefficients, τ and $\dot{\gamma}$ are respectively the shear stress and the shear rate – namely the magnitudes of tensor $\boldsymbol{\tau}$ and **D** – $\mathbf{t}_h$ is the stress vector, $\mathbf{u}_g$, $\boldsymbol{\tau}_g$ and λ_g are the imposed velocity, extra-stress boundary and structure parameter conditions, respectively. In addition, the fluid relaxation time θ, the shear modulus G, the structural viscosity η_v, the steady state of the structure parameter λ_{ss}, the steady state of the viscosity η_{ss} introduced by de Souza Mendes (2009) – with all quantities depending on the structure parameter λ – and the upper-convected time derivative of tensor $\overset{\nabla}{\boldsymbol{\tau}}$ (Astarita and Marrucci, 1974) are given by

$$\theta(\lambda)=\frac{\eta_v(\lambda)}{G(\lambda)} \tag{2}$$

$$G(\lambda)=\frac{G_0}{\lambda^m} \tag{3}$$

$$\eta_v(\lambda)=\left(\frac{\eta_0}{\eta_\infty}\right)^{\lambda}\eta_\infty \tag{4}$$

$$\lambda_{ss}(\dot{\gamma})=\frac{\ln\eta_{ss}(\dot{\gamma})-\ln\eta_\infty}{\ln\eta_0-\ln\eta_\infty} \tag{5}$$

$$\eta_{ss}(\lambda)=\left[1-\exp\left(-\frac{\eta_0\dot{\gamma}}{\tau_0}\right)\right]\left[\frac{\tau_0-\tau_{0_d}}{\dot{\gamma}}e\left(-\frac{\dot{\gamma}_0}{\dot{\gamma}_{0_d}}\right)+\frac{\tau_{0_d}}{\dot{\gamma}}+K\dot{\gamma}^{n-1}\right]+\eta_\infty \tag{6}$$

$$\overset{\nabla}{\boldsymbol{\tau}}=(\nabla\boldsymbol{\tau})\mathbf{u}-\nabla\mathbf{u}\,\boldsymbol{\tau}-\boldsymbol{\tau}\nabla\mathbf{u}^T \tag{7}$$

in which G_0 is the shear modulus of the material totally structured, m is a dimensionless positive scalar, η_0 and η_∞ are the viscosity when the material is either totally structure $(\lambda=1)$ or is unstructured $(\lambda=0)$ respectively, τ_0 and τ_{0_d} are static and dynamic yield stresses respectively, $\dot{\gamma}_{0_d}$ is the shear rate value for which stress transition from τ_0 to τ_{0_d} occurs , K is the consistency index and n is the power-law coefficient.

2.1. A multi-field GLS approximation

A multi-field GLS formulation for structure fluid flows governed by multi-field problem defined by Eq. (1)-(7) can be introduced as: *find the quadruple* $(\boldsymbol{\tau}^h, p^h, \mathbf{u}^h, \lambda^h)\in\boldsymbol{\Sigma}^h\times P^h\times\mathbf{V}_g^h\times\Lambda^h$ *such as:*

$$B(\boldsymbol{\tau}^h, p^h, \mathbf{u}^h, \lambda^h; \mathbf{S}^h, q^h, \mathbf{v}^h, \varphi^h) = F(\mathbf{S}^h, q^h, \mathbf{v}^h, \Phi^h) \quad \forall (\mathbf{S}^h, q^h, \mathbf{v}^h) \in \boldsymbol{\Sigma}^h \times P^h \times \mathbf{V}^h \times \Lambda^h \tag{8}$$

where

$$\begin{aligned}
&B(\boldsymbol{\tau}^h, p^h, \mathbf{u}^h, \lambda^h; \mathbf{S}^h, q^h, \mathbf{v}^h) = (2\eta_p)^{-1}\int_\Omega \boldsymbol{\tau}^h\cdot\mathbf{S}^h\,d\Omega - \int_\Omega \mathbf{D}(\mathbf{u}^h)\cdot\mathbf{S}^h\,d\Omega + \int_\Omega \boldsymbol{\tau}\cdot\mathbf{D}(\mathbf{v}^h)\,d\Omega \\
&+(2\eta_p)^{-1}\int_\Omega \theta(\lambda)(\nabla\boldsymbol{\tau}^h)\mathbf{u}^h\cdot\mathbf{S}^h\,d\Omega - (2\eta_p)^{-1}\int_\Omega \theta(\lambda)\nabla\mathbf{u}^h\boldsymbol{\tau}^h\cdot\mathbf{S}^h\,d\Omega - (2\eta_p)^{-1}\int_\Omega \theta(\lambda)\boldsymbol{\tau}^h\nabla(\mathbf{u}^h)^T\cdot\mathbf{S}^h\,d\Omega \\
&+\int_\Omega \mathbf{u}^h\cdot\nabla\lambda^h\varphi^h\,d\Omega + \int_\Omega t_{eq}^{-1}\left[\sum_{i=1}^{n}\binom{a}{i}\lambda_i^{h^i}\right]\varphi^h\,d\Omega + \int_\Omega t_{eq}^{-1}\left[\left(\frac{\lambda}{\lambda_{ss}}\right)^b\left(\frac{\tau}{\eta_v(\lambda)\dot\gamma}\right)^c\right]\varphi^h\,d\Omega \\
&-\int_\Omega t_{eq}^{-1}\left[\sum_{i=1}^{n}\binom{a}{i}\lambda_{ss}^i\left(\frac{\lambda^h}{\lambda_{ss}}\right)^b\left(\frac{\tau}{\eta_v(\lambda)\dot\gamma}\right)^c\right]\varphi^h\,d\Omega - \int_\Omega p\,\mathrm{div}\,\mathbf{v}^h\,d\Omega - \int_\Omega \mathrm{div}\,\mathbf{u}^h q^h\,d\Omega \\
&+\int_\Omega \delta(\mathrm{Re}_K)\mathrm{div}\,\mathbf{u}^h\,\mathrm{div}\,\mathbf{v}^h\,d\Omega + \sum_{K\in\Omega^h}\int_{\Omega_K}(\nabla p^h - \mathrm{div}\,\boldsymbol{\tau})\cdot\alpha(\boldsymbol{x})(-\nabla q^h + \mathrm{div}\,\mathbf{S}^h)\,d\Omega + \epsilon\int_\Omega p^h q^h\,d\Omega \\
&+2\eta_p\int_\Omega((2\eta_p)^{-1}\boldsymbol{\tau}^h + (2\eta_p)^{-1}\theta(\lambda)((\nabla\boldsymbol{\tau}^h)\mathbf{u}^h - \nabla\mathbf{u}^h\boldsymbol{\tau}^h - \boldsymbol{\tau}^h\nabla(\mathbf{u}^h)^T) + \mathbf{D}(\mathbf{u})^h)\ \mathrm{x} \\
&\qquad \mathrm{x}\ \beta(\mathrm{De}_K)((2\eta_p)^{-1}\mathbf{S}^h + (2\eta_p)^{-1}\lambda((\nabla\mathbf{S}^h)\mathbf{u}^h - \nabla\mathbf{u}^h\mathbf{S}^h - \mathbf{S}^h\nabla(\mathbf{u}^h)^T) - \mathbf{D}(\mathbf{v})^h)\,d\Omega \\
&+\int_\Omega\left[\mathbf{u}^h\cdot\nabla\lambda^h + \sum_{i=1}^{n}\binom{a}{i}\lambda_i^{h^i} + \left(\frac{\lambda^h}{\lambda_{ss}}\right)^b\left(\frac{\tau}{\eta_v(\lambda)\dot\gamma}\right)^c - \sum_{i=1}^{n}\binom{a}{i}\lambda_{ss}^i\left(\frac{\lambda^h}{\lambda_{ss}}\right)^b\left(\frac{\tau}{\eta_v(\lambda)\dot\gamma}\right)^c\right]\ \mathrm{x} \\
&\qquad \mathrm{x}\ \psi(\boldsymbol{x})\left[\mathbf{u}^h\cdot\nabla\lambda^h + \sum_{i=1}^{n}\binom{a}{i}\varphi_i^{h^i} + \left(\frac{\varphi^h}{\lambda_{ss}}\right)^b\left(\frac{\tau}{\eta_v(\lambda)\dot\gamma}\right)^c - \sum_{i=1}^{n}\binom{a}{i}\lambda_{ss}^i\left(\frac{\varphi^{\hat h}}{\lambda_{ss}}\right)^b\left(\frac{\tau}{\eta_v(\lambda)\dot\gamma}\right)^c\right]d\Omega
\end{aligned} \tag{9}$$

and

$$\begin{aligned}
&F(\mathbf{S}^h, q^h, \mathbf{v}^h, \varphi^h) = \int_\Omega \mathbf{f}\cdot\mathbf{v}^h\,d\Omega + \int_\Omega t_{eq}^{-1}\varphi^h\,d\Omega + \int_{\Gamma_h}\mathbf{t}_h\cdot\mathbf{v}^h\,d\Gamma + \sum_{K\in\Omega^h}\int_{\Omega_K}\mathbf{f}\cdot\alpha(\boldsymbol{x})(-\nabla q^h + \mathrm{div}\,\mathbf{S})\,d\Omega \\
&+\sum_{K\in\Omega^h}\int_{\Omega_K} t_{eq}^{-1}\psi(\boldsymbol{x})\left[\mathbf{u}^h\cdot\nabla\lambda^h + \sum_{i=1}^{n}\binom{a}{i}\varphi_i^{h^i} + \left(\frac{\varphi^h}{\lambda_{ss}}\right)^b\left(\frac{\tau}{\eta_v(\lambda)\dot\gamma}\right)^c - \sum_{i=1}^{n}\binom{a}{i}\lambda_{ss}^i\left(\frac{\varphi^{\hat h}}{\lambda_{ss}}\right)^b\left(\frac{\tau}{\eta_v(\lambda)\dot\gamma}\right)^c\right]d\Omega
\end{aligned} \tag{10}$$

with $\Lambda^h \times \boldsymbol{\Sigma}^h \times P^h \times \mathbf{V}_g^h$ *is the finite element space product for structure parameter, extra-stress, pressure and velocity, respectively, and the stability parameter* $\alpha(\boldsymbol{x})$, $\beta(Wi_k)$ *and* $\psi(\boldsymbol{x})$ *taken as extensions of the ones introduced by Franca and Frey (1992) and Behr et al. (1993) for constant viscosity fluids.*

3. NUMERICAL RESULTS

In this section, some GLS simulations of structured fluid flows are undertaken. The structured fluid flows around a cylinder – of radius *R* – that is confined to a planar channel of height *H*, .with the geometry presenting an aspect ration *H*/*R* ratio equal to 1:8 – see Fig. 1 for a detailed geometry and problem statement. The kinematic boundary conditions are the following: (i) no-slip and impermeability on channel wall and on the cylinder surface; (ii) symmetry conditio $(\partial_{x_2}u_1 = u_2 = \tau_{12} = 0)$ on channel centerline – since only half the channel is considered on numerical tests; (iii) inlet fully-developed viscoelastic profiles for velocity and extra-stress,

$$\begin{aligned}
&u_1^- = 1.5\,\overline{u}^-(1 - x_2^2/H^2)\ ;\ u_2^- = 0 \\
&\tau_{12}^- = \eta_p(-3\,x_2/H^2)\ ;\ \tau_{11}^- = 2\,\theta\,\eta_p(-3\,x_2/H^2)^2\ ;\ \tau_{22}^- = 0
\end{aligned}\ ; \tag{11}$$

and free-traction $([-p\mathbf{1} + \boldsymbol{\tau}]\mathbf{n} = \mathbf{0})$ at channel outlet. For the evolution equation of the structure parameter, the following boundary condition are imposed: (i) unitary uniform profile at inlet channel; (ii) and, on all boundaries, null multi-directional gradients are prescribed, $\nabla\lambda\cdot\mathbf{n} = 0$.

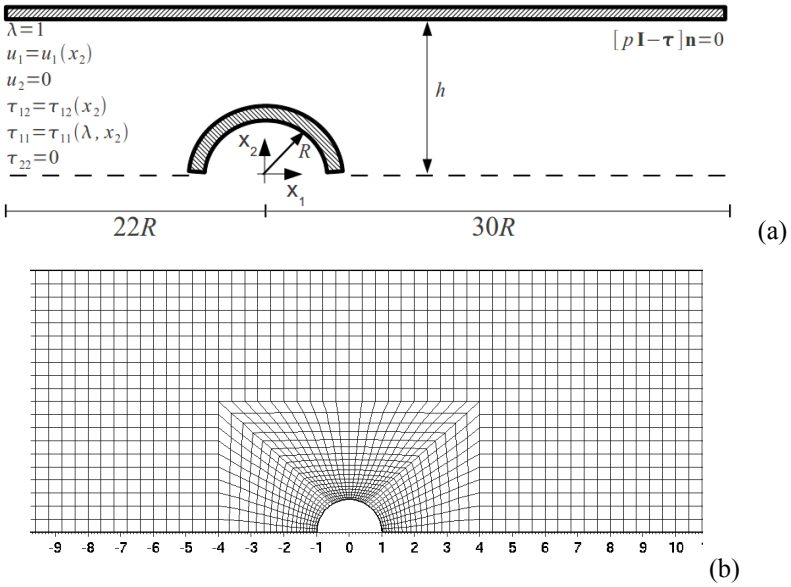

Figure 1. Structure flow around a cylinder: (a) the problem statement; (b) a mesh detail.

The boundary conditions are (i) no-slip and impermeability on channel walls and cylinder surface, (ii) velocity and extra-stress symmetry conditions on the centerline, and (iii) fully-developed velocity and extra-stress profiles at inflow and outflow.

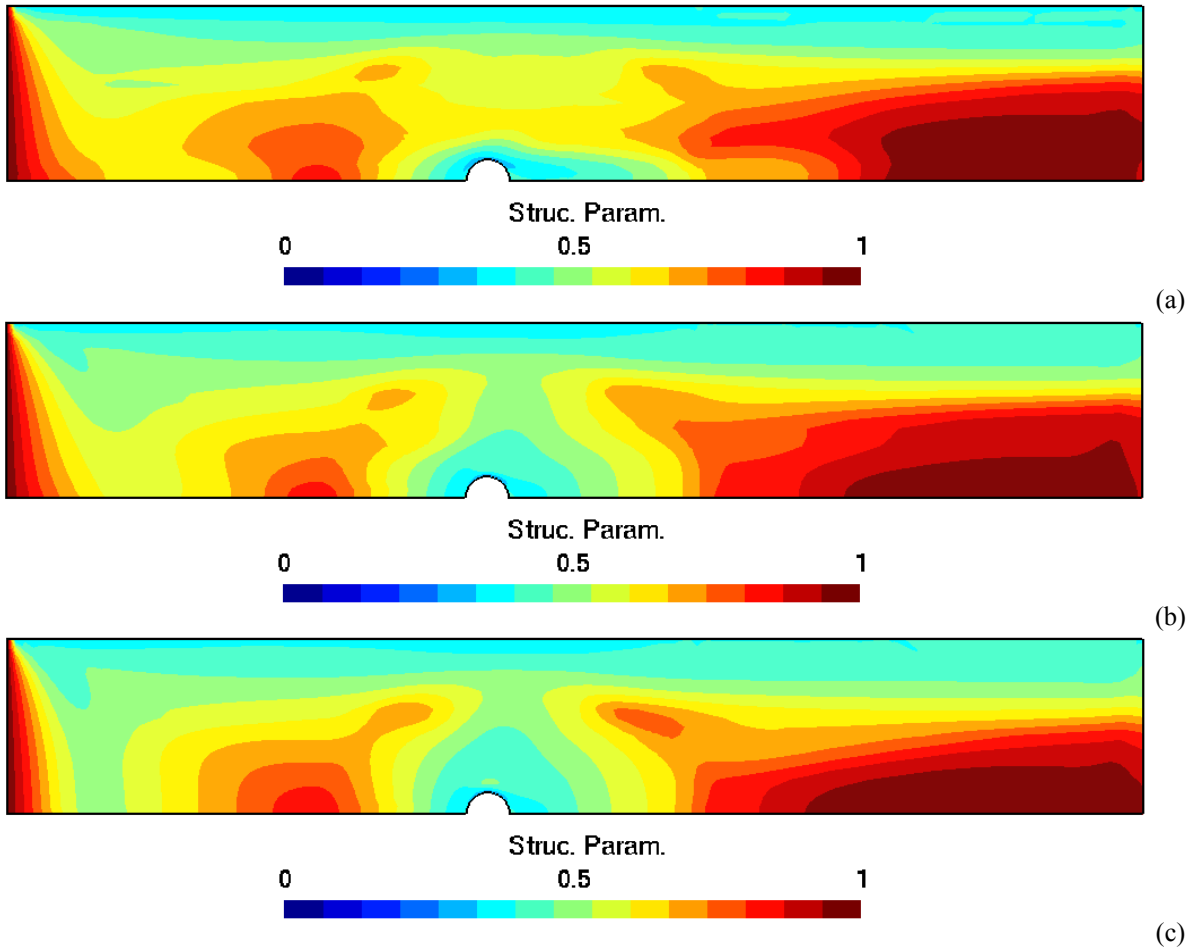

Figure 2. Structure Parameter iso-bands: (a) G_0=2 Pa; (b) G_0=10 Pa; (c) G_0=100 Pa.

Figures 2 shows structure parameter isobands throughout the channel, for G_0=2-100 Pa, t_{eq}=1s, U=1 m/s, n=0.5, K=1 Pa.s^n $\tau_0=2\,\text{Pa}$, $\tau_{0_d}=1\,\text{Pa}$, $\eta_0=10^4\,\text{Pa.s}$, $\eta_\infty=10^{-2}\,\text{Pa.s}$, m=0.1, a=b=1.0 e c=0.1. It can be noted highly

structured regions – that is to say regions subjected to values of λ close to unity – at channel inlet and around the centerline. In contrast, regions subjected to low values of λ can be found near the channel walls and close the cylinder. In addition, as the shear modulus increases, from 2 Pa up to 100 Pa, the structured material regions tend to decrease and conversationally the unstructured regions tend to increase. The topology of the unstructured material regions can be explained by the collapse of the material zones due to higher strain rates. Secondly, the monotonically increasing of the unstructured regions with G_0 is due to the low degree of the fluid elasticity for such a situation; from the modified UCM viscoelastic equation (Eq. (1) and (2)), the more the shear modulus increases, the more the upper-convected derivative of extra-stress decreases.

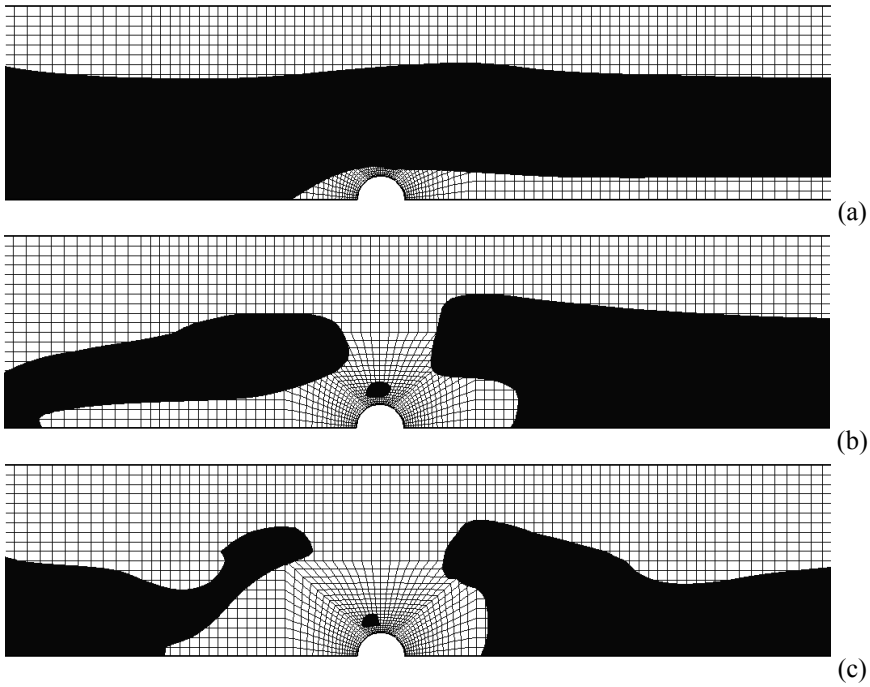

Figure 3. A blown-up view of unyielded regions around the cylinder: (a) G_0=2 Pa; (b) G_0=10 Pa; (c) G_0=100 Pa.

In Fig. 3, the unyielded material regions for the flows illustrated in Fig. 2 are shown. It is worth noting a strong linking between both figures. For G_0=2 Pa – the most elastic case – it can clearly be noticed a high-λ-structure region (yellow zone) throughout the channel (see Fig. 2a) corresponding to an unyielded region in Fig. 3a. For G_0=10 Pa and 100 Pa, the same behavior repeats itself; unyielded regions in Fig. 3b and 3c can be related to similar (topology) unstructured regions in Fig. 2b and 2c. This linkage is expected since the elastic unstructured region are subjected to lower shear stresses and consequently the material can not overcame its yield limit. Yet the material is considerably unstructured, the stresess acting upon it are higher and it can flow as a power-law fluid.

4. FINAL CONCLUSION

In this work a multi-field GLS approximation for upper-convected Maxwell model is used to analyze the creeping flow of a thixotropic fluid around a cylinder between two parallel plates. The effect of the shear modulus on the structure parameter and on the flow pattern is presented and discussed. The geometry is held fixed and inertia is neglected. The results obtained show that for highly elastic fluids (lower shear modulus G_0) larger regions of structured (elastic) and unyielded fluid are found. Increasing the shear modulus it is observed that some structured regions are broken and yielded zones appear close to the cylinder wall. These preliminary results indicate that the model is valid to predict the behavior of thixotropic fluids, since all results are physically meaningful and in accordance with the related literature. However, further tests are being performed to confirm and validate the model.

5. ACKNOWLEDGEMENTS

The author C. Fonseca thanks for his graduate scholarship provided by CAPES and the authors S. Frey and M. Naccache acknowledges CNPq for financial support.

6. REFERENCES

Astarita, G. Marrucci, G., 1974, “Principles of Non-Newtonian Fluid Mechanics”. McGraw-Hill, Great Britain.
Barnes, H.A., 1997. “Thixotropy-a review”. J. of Non-Newt. Fluid Mechanics, Vol. 70, p. 1-33.
Behr, M., Franca, L.P., Tezduyar, T.E., 1993. “Stabilized Finite Element Methods for the Velocity-Pressure-Stress Formulation of Incompressible Flows”, Comput. Methods Appl. Mech. Engrg., Vol. 104, pp. 31-48.
De Souza Mendes, P. R., 2009, “ Modelling the thixotropic behavior of structured fluids”. J. of Non-Newt. Fluid Mechanics, Vol. 164, p. 66-75.
Franca, L. P., Frey, S., 1992, “Stabilized Finite Element Methods: II. The Incompressible Navier-Stokes Equations”. Computer Methods in Applied Mechanics and Engineering, 99, pp. 209-233.
Mewis, J. and Wagner, N.J., 2009. “Thixotropy”. Adv. Colloid Interface Sci., Vol. 147-148, p. 214-227.

7. RESPONSIBILITY NOTICE

The authors are the only responsible for the printed material included in this paper.